




Article

Precipitated K-Promoted Co–Mn–Al Mixed Oxides for Direct NO Decomposition: Preparation and Properties

Květa Jiráto^{1,*}, Kateřina Pacultová² , Jana Balabánová¹, Kateřina Karásková², Anna Klegová², Tereza Bílková², Věra Jandová¹, Martin Koštejn¹, Alexandr Martaus², Andrzej Kotarba³  and Lucie Obalová² 

¹ Institute of Chemical Process Fundamentals of the CAS, v.v.i., Rozvojová 135, CZ- 165 02 Praha 6- Suchbát, Czech Republic

² Institute of Environmental Technology, VŠB- TU Ostrava, 17. listopadu 15/2172, CZ- 708 00 Ostrava- Poruba, Czech Republic

³ Faculty of Chemistry, Jagiellonian University, Gronostajowa 2, PL- 30387 Krakow, Poland

* Correspondence: jiratova@icpf.cas.cz

Received: 28 May 2019; Accepted: 5 July 2019; Published: 9 July 2019



Abstract: Direct decomposition of nitric oxide (NO) proceeds over Co–Mn–Al mixed oxides promoted by potassium. In this study, answers to the following questions have been searched: Do the properties of the K-promoted Co–Mn–Al catalysts prepared by different methods differ from each other? The K-precipitated Co–Mn–Al oxide catalysts were prepared by the precipitation of metal nitrates with a solution of K₂CO₃/KOH, followed by the washing of the precipitate to different degrees of residual K amounts, and by the calcination of the precursors at 500 °C. The properties of the prepared catalysts were compared with those of the best catalyst prepared by the K-impregnation of a wet cake of Co–Mn–Al oxide precursors. The solids were characterized by chemical analysis, DTG, XRD, N₂ physisorption, FTIR, temperature programmed reduction (H₂-TPR), temperature programmed CO₂ desorption (CO₂-TPD), X-ray photoelectron spectrometry (XPS), and the species-resolved thermal alkali desorption method (SR-TAD). The washing of the K-precipitated cake resulted in decreasing the K amount in the solid, which affected the basicity, reducibility, and non-linearly catalytic activity in NO decomposition. The highest activity was found at ca 8 wt.% of K, while that of the best K-impregnated wet cake catalyst was at about 2 wt.% of K. The optimization of the cake washing conditions led to a higher catalytic activity.

Keywords: NO decomposition; Co–Mn–Al mixed oxides; catalyst preparation; potassium promoter

1. Introduction

Nitric oxide (NO) is considered a harmful gas, as it negatively affects the environment by attenuating the ozone layer and contributing to the formation of acid rain and smog [1]. NO is formed by natural processes and anthropogenic activity. This paper is focused on studies of the catalytic processes devoted to the removal of nitrogen oxide from stationary exhaust sources. In principle, primary or secondary methods can be used for NO_x emissions abatement. Primary methods aim to prevent NO_x formation during combustion processes. Secondary methods reduce the concentration of the already formed NO_x. The most commonly used secondary methods include selective non-catalytic reduction (SNCR) and selective catalytic reduction (SCR) [2,3]. The SNCR proceeds without the presence of a catalyst, but requires high reaction temperatures (above 850 °C) to meet the high efficiency of the process. Such conditions can be achieved in laboratories, but it is not easy to meet them at real industrial conditions, because there are many factors influencing them, and, thus, it is difficult to maintain the

SNCR process constant [4]. On the other hand, SCR proceeds at much lower temperatures (200–450 °C) but needs the presence of a catalyst. The disadvantage of the SCR method is the need to use a reducing agent, most often ammonia and urea [5]. The use of a reducing agent increases operating costs, and the process may be accompanied by unwanted emissions of unreacted reducing agents or other reaction by-products. Moreover, in the case of ammonia storage, strict safety measures are required.

The direct decomposition of nitric oxide has been studied and described in some publications [6]. Apart from metals (Pt, Pd, Ag, Rh, Ni, Cu, Mo, Co, Au), metal oxides like Co_3O_4 , Fe_2O_3 , NiO, CuO, and ZrO_2 ; lanthanides; perovskites; and mixed oxides were also studied for direct NO decomposition [7–10]. A Co_3O_4 catalyst alkalized by a small amount of Li, Na, K, Rb, or Cs showed higher NO conversion than non-promoted Co_3O_4 . Alkali metals were added by the impregnation method, and from all investigated promoters, potassium showed the best results [11].

Alkali metals are often used in the preparation of heterogeneous catalysts for their ability to modify structural and/or the electronic properties of metal oxides [12,13]. It is known [14] that potassium adsorption on metal surfaces results in the dominant lowering of the surface potential on sites adjacent to a potassium atom and a small, but still significant, lowering of the potential on sites located further away.

As shown in [5], the method of catalyst preparation affects its activity and stability. Pacultova et al. [15] found out that potassium modified Co–Mn–Al mixed oxide catalysts prepared from hydrotalcite-like precursors could efficiently catalyze the decomposition reaction, as it proceeds successfully in the temperature region of 600–700 °C. The durability of the activity of the catalyst can be influenced by stability of potassium in the catalysts at the applied reaction conditions. The co-precipitation of metal nitrates by a $\text{Na}_2\text{CO}_3/\text{NaOH}$ water solution and subsequent impregnation of the resulting wet cake by KNO_3 solution (the K-impregnation of wet cake is labeled as BP) led to a higher activity and stability of the catalyst than the other examined methods, like the impregnation of the calcined Co–Mn–Al precursor with a solution of KNO_3 or the calcination of corresponding metal nitrates. A rather complicated preparation procedure is main disadvantage of the preparation method consisting in metal salt co-precipitation by solutions of Na compounds and following the impregnation of a cake with K salts.

In the paper of Yongzhao Wang et al. [16], cobalt–cerium mixed oxides modified by K were prepared by the co-precipitation of a metal nitrates solution with an aqueous solution of K_2CO_3 and/or KOH, and the catalysts were used in a deN_2O process.

We believe that the incorporation of potassium into the structure of catalyst particles would affect catalytic activity and stability in direct NO decomposition. The main objective of our study was the enhancement of the NO catalytic decomposition rate through the optimization of the preparation methods. Results obtained in this study have confirmed that the precipitation of Co, Mn, and Al nitrates with a $\text{K}_2\text{CO}_3/\text{KOH}$ solution is a promising preparation method that provides a uniform distribution of the promoter (potassium) in the catalyst particles, appropriate catalyst basicity, and reducibility and slightly higher catalytic activity in direct NO decomposition.

2. Results

In this chapter, the authors describe the experimental results obtained with the Co–Mn–Al mixed oxide catalysts containing variable concentrations of potassium prepared by the gradual washing of precipitates of Co, Mn, and Al nitrate solutions with a $\text{K}_2\text{CO}_3/\text{KOH}$ solution, and they compare them with the catalyst prepared by the K-impregnated wet cake Co–Mn–Al mixed oxide catalyst. The precursors and the catalysts were characterized by chemical analysis, differential thermogravimetry (DTG), XRD, N_2 physisorption, FTIR, H_2 -TPR, CO_2 -TPD, XPS, and the thermal alkali desorption method (SR-TAD), and their catalytic activity was evaluated in direct decomposition of NO.

2.1. Properties of the Dried Samples

Samples of dried Co–Mn–Al catalyst precursors modified with various amount of potassium were prepared by washing the precipitates. The process of precursor washing and filtration is described in

detail in Supplementary Table S1. The wet cake of the catalyst precursor obtained by precipitation was gradually washed with demineralized water to obtain five samples with decreasing concentrations of potassium. One fifth of the original cake was removed and left to dry, and the remaining part of the cake was washed with 200 ml of water and filtered again. The procedure was repeated four times to obtain samples “1” to “5” with a gradual decrease of K concentration. In addition to potassium, small amounts of Na was found in the filtrates, most likely originating from the initial compounds used for catalyst preparation.

2.1.1. Phase Composition

X-ray diffraction is the main technique for the investigation of bulk structure, which is very important, as many of the catalyst characteristics depend on it. XRD measurements were used to characterize the dried catalysts precursors. The diffraction patterns of the precipitated samples dried at 60 °C confirmed the presence of a hydrotalcite-like compound (H) with peak maxima at 13.3, 27.0, 40.2, 41.3, 45.6, 70.9, and 72.9° (ICDD PDF-2 card No. 01-070-2151) and manganese carbonate (rhodochrosite R) with peaks maxima at 28.1, 36.6, 43.8, 48.4, 53.0, 58.4, 60.7, and 80.6° (ICDD PDF-2 card No. 00-007-0268) (Supplementary data, Figure S1). The gradual washing of the precursors and therefore, the decreasing K concentration, led to the continuous crystallization of the hydrotalcite-like compounds, manifesting itself in higher peaks of hydrotalcite. A slightly lower intensity of the basal (003) and (006) diffraction patterns (detected in the range of 2Theta from 10 to 30°) in comparison with non-basal patterns can indicate a lower concentration of preferably orientated layered double hydroxide (LDH) crystals. Apart from hydrotalcite, a K compound (KNO₃) at 2Theta 21.95, 34.07, 37.7, 39.55, 48.12, and 54.5 (°) was detected in two samples (“1” and “2”) with the highest K concentration. Though K₂CO₃/KOH was used as the precipitant, KNO₃ was formed during precipitation in the solution by the recombination of ions (metal nitrates were used for catalyst preparation). A decreasing concentration of K in the samples led to the gradual diminution of peaks characteristic for K components in the diffractogram. Nevertheless, a small part of the most intensive peak at 2Theta = 54.5 (°) remained preserved, except for the “5” sample, in which a very low concentration of K was determined.

2.1.2. TG and DTG Measurements

Thermogravimetry (TG) and differential thermogravimetry (DTG) measurements of the dried “1”–“5” samples showed (Table 1) three areas of maximum weight decrease manifesting in the ranges of 113–136, 193–213, and 448–558 °C. With decreasing K concentration in the mixed transition metal precursors, the position of the peaks shifted slightly to lower temperatures.

The weight change between 193–213 °C was the most significant (ca 13.5–18%). A somewhat smaller weight decrease (9.5–13.9%) was observed in the stage appearing at the lowest temperatures (113–136 °C). The weight loss in the high temperature region (438–558 °C) was the smallest and varied from 1.5 to 3.7%.

Table 1. Results of thermogravimetry (TG) and differential thermogravimetry (DTG) measurements of the dried samples.

Sample	DTG_1 <i>T</i> _{max} , °C	DTG_2 <i>T</i> _{max} , °C	DTG_3 <i>T</i> _{max} , °C	ΔTG_1 %	ΔTG_2 %	ΔTG_3 %
“1”	113	201	558	−9.5	−17.4	−3.7
“2”	131	206	Nd ^a	−11.9	−14.8	−2.7
“3”	132	201	438	−11.6	−14.0	−3.2
“4”	136	213	445	−13.9	−18.4	−1.5
“5”	136	193	448	−13.7	−13.5	−3.6

^a Not detected.

To identify the processes taking place in various temperature regions during the temperature treatment of catalyst precursors, an analysis of effluents by mass spectroscopy was carried out during calcination. Three selected precursors differing in K concentration were calcined in helium (0.1 g, temperature ramp 20 K min^{-1}), and the results are shown in Figure 1. Desorption of H_2O was finished at ca $500 \text{ }^\circ\text{C}$, with temperature maxima at ca 187 and $250 \text{ }^\circ\text{C}$.

The decomposition of nitrates in the catalysts proceeds in two steps, manifesting as a presence of NO and NO_2 in the gas phase. A higher concentration of NO than NO_2 was observed for the catalysts with a K concentration higher than 1 wt.%. Carbonates present in the precursors were decomposed in three stages, the first one (at ca $140 \text{ }^\circ\text{C}$) being of lowest intensity. The course of the two following regions (at ca 250 and $400 \text{ }^\circ\text{C}$) changed in dependence on K concentration: With a lower K concentration, the temperature maxima shifted slightly to higher temperatures. It is very likely that oxyhydroxides decompose first, and K_2CO_3 , which remains in the catalysts as a residue of the precipitating agent, decomposes at about $400 \text{ }^\circ\text{C}$. The positions of all temperature peak maxima are summarized in Table 2.

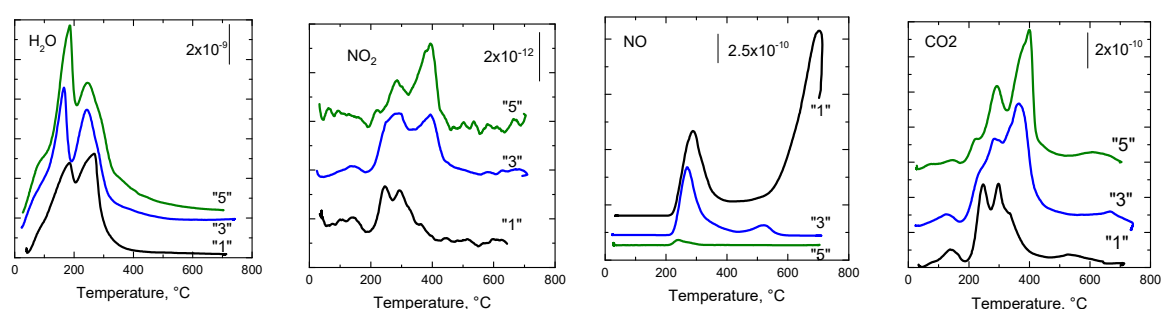


Figure 1. Composition of effluents in A observed by mass spectroscopy during calcination of the “1”, “3”, and “5” samples in helium (0.2 g of sample, 20 K min^{-1}).

Table 2. Positions of the temperature peak maxima ($^\circ\text{C}$) observed during calcination of the selected precursors in helium.

Sample	H_2O	NO_2	NO	CO_2
“1”	184; 269	126; 242; 293	287; 702	144; 249; 297; 535
“3”	164; 245	139; 274; 400	272; 520	136; 289; 366; 668
“5”	95; 187; 245	106; 281; 400	242	148; 229; 290; 400; 628

It can be concluded that the first peak in the DTG measurements can be ascribed to the removal of water, the second one to the decomposition of carbonates and nitrates present in the metal oxyhydroxides, and the third one to the decomposition of carbonates and nitrates present in the precipitates as compounds.

2.2. Properties of the Calcined Precursors

2.2.1. Chemical Composition

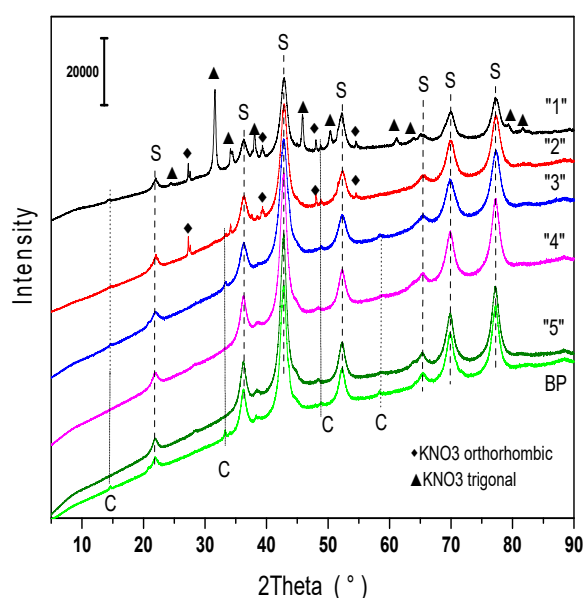
The chemical compositions of the catalysts calcined for 4 h at $500 \text{ }^\circ\text{C}$ are shown in Table 3. Potassium concentration gradually decreased due to washing from 18.9 to 0.6 wt.%. All catalysts, except the one with the highest K concentration, showed molar ratios closely approaching that of the average formula $\text{Co:Mn:Al} = 4:1.4:1.3$. However, the molar ratio of K to Co decreased from the value of 4 for sample “1” to 0.1 for sample “5”. The molar ratio of the K-impregnated wet cake catalyst (BP) approached that of the sample “3”.

Table 3. Composition of the samples calcined 4 h at 500 °C determined by chemical analysis and molar ratios of the metals.

Sample	Wt.%				Molar Ratio
	K	Co	Mn	Al	Co:Mn:Al:K
"1"	18.90	28.2	6.0	3.0	4:0.9:0.9:4.0
"2"	8.20	40.0	8.8	4.0	4:1.3:1.2:1.7
"3"	2.39	45.4	10.2	4.7	4:1.5:1.5:0.5
"4"	0.92	46.8	10.2	4.7	4:1.6:1.5:0.2
"5"	0.60	45.6	9.9	4.4	4:0.9:1.4:0.1
BP	2.10	48.9	11.2	5.1	4:0.9:1.5:0.4

2.2.2. Phase Composition

The XRD patterns (Figure 2) of the precursors calcined for 4 h at 500 °C exhibited a Co_3O_4 spinel-like structure (labelled as S), which was dominant in all examined samples. Diffraction positions at 21.9, 36.3, 42.7, 52.3, 65.4, 69.8, and 77.2° and the intensity of the peaks are in agreement with the data published for this system (ICDD PDF-2 card No 01-074-1656). Traces of cryptomelane $\text{KMn}_8\text{O}_{16}$ (ICDD PDF-2 card No 00-006-0547), labelled as C in the diffractograms overlay, seemed to be present in all calcined samples, especially in those having higher K concentration (the "1", "2", and "3" samples). Qihua Zhang et al. [17] identified cryptomelane in the calcined precursor formed by a reaction of KMnO_4 and maleic acid at moderate temperatures (300–600 °C). At temperatures above 600 °C, cryptomelane usually transforms into bixbyite (Mn_2O_3), but in the prepared samples, such compound was not detected. Except for the above mentioned phases, the peaks at 27.26, 39.17, 48.0, and 54.65 appeared in diffractograms that were ascribed to potassium nitrate (KNO_3) in trigonal crystallographic modification (ICDD PDF-2 card No 01-078-7937). A somewhat lower concentration of the orthorhombic modification of KNO_3 was registered at 24.3, 31.55, 34.29, 38.0, 45.79, 50.37, 61.25, 63.91, 79.37, and 81.71° (ICDD PDF-2 card No 01-074-2055) in samples "1" and "2", which were washed only partly. It is also obvious from diffractograms that the examined samples with a higher stage of washing showed better crystallinity than those only partly washed.

**Figure 2.** Diffraction patterns of the calcined K-precipitated Co–Mn–Al precursors containing various amounts of potassium. S—spinel, ▲— KNO_3 trigonal, ◆— KNO_3 orthorhombic, C— $\text{KMn}_8\text{O}_{16}$ cryptomelane.

The effect of potassium concentration in the Co–Mn–Al oxides on spinel lattice parameter a and spinel coherent domains L_d can be seen in Table 4 and Figure 3, respectively. The crystallite size of the spinel was calculated using Scherrer's formula from the following diffraction lines (220), (311), (400), (511), and (440). The calculated value was corrected to the instrumental broadening (NIST SRM 660b). Recently, Kovanda et al. [18] described the behavior of potassium non-modified Co–Mn–Al mixed oxides during calcination. They found out that the decomposition of Co–Mn–Al layered double hydroxides above 200–260 °C proceeds with the formation of nanocrystalline spinels, and spinels are the only phases present up to 900 °C. At a temperature of about 500 °C, the segregation of the Co-rich spinel was observed, while the incorporation of manganese into the spinel lattice proceeded during its further recrystallization, and this process was accompanied by a lattice parameter decrease. The presence of potassium in Co–Mn–Al oxides could also affect the lattice parameter a of the spinel: One can imagine that in case of no potassium or just a small amount of it in the oxides, manganese enters into the spinel lattice during calcination and decreases the lattice parameter due to the partial distortion of the Co_3O_4 lattice. With an increasing amount of potassium in the sample, more manganese is bonded to potassium, and, therefore, manganese cannot enter the Co spinel lattice, which is why the spinel lattice parameter a could return to the values characteristic of the Co_3O_4 phase [19]. However, it is obvious from Table 4 that the presence of the increasing amount of potassium in the K-precipitated Co–Mn–Al oxides caused only small changes (± 0.001 nm, less than 0.2 rel.%) in the lattice parameter of the spinel.

The dimension of the spinel coherent domain L_d appears to decrease from 9 to 6 nm when the K concentration increases to 2.4 wt.%. With a further increase of K concentration in the solids, the spinel coherent domain started increasing and reached the value of 9 nm at a K concentration equal to 18.9 wt.% (Figure 3). The course of the dependence seems to correspond to the changes in spinel lattice parameter, but the differences among L_d parameters were very small—the observation of the minimum in the dependence could be coincidental.

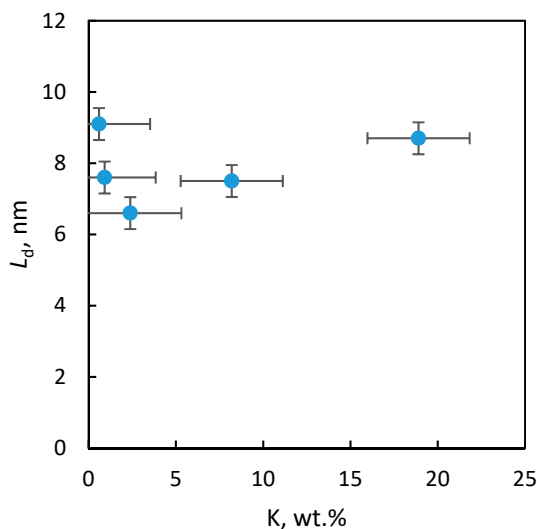


Figure 3. Dependence of spinel coherent domain L_d on concentration of K in the K-precipitated Co–Mn–Al mixed oxides catalysts.

2.2.3. Textural Properties

The porous structure of the K-precipitated catalysts was characterized by the adsorption/desorption of nitrogen at -196 °C, and the results are summarized in Table 4. The surface area of the catalysts S_{BET} with a concentration of potassium lower than 2.4 wt.% was about $100 \text{ m}^2 \text{ g}^{-1}$. A higher concentration of potassium in the samples caused a diminution of surface area; the smallest surface was exhibited by the catalyst with 18.9 wt.% K ($S_{\text{BET}} < 1 \text{ m}^2 \text{ g}^{-1}$). Accordingly, total pore volume increased with

the decreasing K concentration in the solids from 266 to 435 mm³_{liq}/g. The volume of micropores was small in all cases (less than 5% of total pore volume). The experimental data document that the concentration of potassium in the catalyst higher than 8 wt.% had a negative effect on the porous structure of metal oxides. The phenomenon is likely connected with the collapsing of smaller pores and coalescence of larger pores.

Table 4. Characteristic physical–chemical data of the samples calcined 4 h at 500 °C.

Sample	S_{BET} (m ² /g)	S_{meso} (m ² /g)	V_{tot} (mm ³ _{liq} /g)	V_{micro} (mm ³ _{liq} /g)	L_d (nm)	a (nm)
"1"	<1	–	–	–	9	$0.81056 \pm 7 \times 10^{-5}$
"2"	58	32	266	13	8	$0.81187 \pm 17 \times 10^{-5}$
"3"	110	69	401	22	7	$0.81109 \pm 5 \times 10^{-5}$
"4"	105	66	435	21	8	$0.81209 \pm 4 \times 10^{-5}$
"5"	102	66	435	21	9	$0.81153 \pm 4 \times 10^{-5}$
BP	94	Nd. *	460	64	9	$0.81015 \pm 4 \times 10^{-5}$

* Not determined.

The adsorption–desorption isotherms of nitrogen (Figure S2 in Supplementary data) obtained over calcined catalysts confirm that there was not a large difference in pore size distribution among the catalysts with a potassium concentration lower than 2.4 wt.%.

2.2.4. Reducibility

The reducibility of the catalysts with different contents of potassium was studied by H₂-TPR in the temperature range of 25–900 °C. The H₂-TPR patterns of the K-precipitated catalysts are depicted in Figure 4. The catalysts were reduced in two main temperature regions, 200–500 °C and >500 °C. The low-temperature reduction peak represents the reduction of Co^{III} → Co^{II} → Co⁰ in the Co₃O₄-like phase and the reduction of Mn^{IV} to Mn^{III} oxides. The reduction of Mn^{III} → Mn^{II} can take place in both temperature regions [19]. The reduction of the K containing compounds, like cryptomelane KMn₈O₁₆ or others, also cannot be excluded in the low temperature region since the reduction of those species proceeds at temperatures between 200–450 °C [20–23]. In literature, the high temperature peak was ascribed to the reduction of Co and Mn ions surrounded by Al ions in the spinel-like phase [24] and to the reduction of Mn^{III}. The effect of K amount on reducibility in the fresh samples, calcined at 500 °C, is shown in Figure 4. The modification of the Co–Mn–Al mixed oxide by potassium caused significant changes in the obtained reduction profiles. With an increasing K content, a shift to lower temperatures accompanied by the broadening of the peak was observed. A new low temperature peak appeared as a shoulder at around 300 °C. The catalyst with the highest concentration of K (sample "1") was completely reduced in the temperature region 200–500 °C, while all the other catalysts showed a high-temperature reduction peak with a maximum between 614 and 755 °C. The temperature 755 °C was determined for the catalyst with the lowest K concentration. The position of the temperature peak maximum shifted to lower temperatures with increasing K concentration, reaching the value of 614 °C for sample "2". Thus, the positions of T_{max} of the reduction peaks in H₂-TPR (Table 5) reflected the concentration of K in the catalysts: Increasing the concentration of K (except the highest concentration 18.9 wt.%) led to the easier reduction of the metal mixed oxides. The reduction profile of the catalyst prepared by modified by impregnation of wet cake (BP) was similar as that of the sample "5".

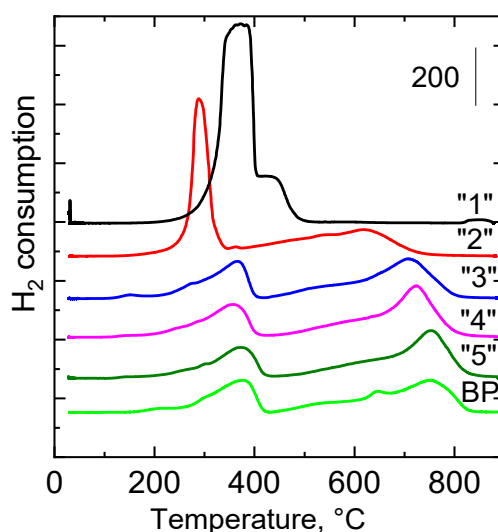


Figure 4. H₂-TPR profiles of the samples with different amount of K, calcined for 4 h at 500 °C.

Table 5. Positions of the peak maxima in TPR curves and consumptions of hydrogen and CO₂ in H₂-TPR and CO₂-TPD measurements, respectively.

Sample	H ₂ -TPR <i>T</i> _{max} , °C	H ₂ -TPR ^a mmol g ⁻¹	CO ₂ -TPD <i>T</i> _{max} , °C	CO ₂ -TPD ^a mmol g ⁻¹
"1"	376; 438 ^b	18.24	-	0.03
"2"	290; 614	12.62	120; 275; 444	0.18
"3"	362; 709	6.61	101; 203; 350	0.16
"4"	368; 726	6.29	101; 202	0.09
"5"	371; 756	5.67	101; 202	0.10
BP	375; 755	6.82	105; 277; 630	0.16

^a in the range of 25–650 °C, ^b shoulder.

2.2.5. Basicity

Catalyst basicity is an important factor influencing the chemical reactivity of NO because of the acidic nature of the NO molecule [25]. In the CO₂-TPD profiles of mixed oxides catalysts, several types of basic sites can be recognized. Weak basic sites are attributed to –OH groups occurring on the surface of the catalyst, medium sites consist of oxygen bonded to metal as Me²⁺-O²⁻ or Me³⁺-O²⁻ pairs, and strong basic sites are assigned to isolated O²⁻ anions [26]. Individual peaks below 140 °C can be ascribed to weak basic sites, the peaks appearing in the range of 140–220 °C can be assigned to medium basic sites, and the peaks above 270 °C can be assigned to strong basic sites.

TPD-CO₂ measurements were performed with the aim to find differences in basicity of the fresh catalysts calcined at 500 °C. The effect of potassium content on the amount of basic sites is shown in Figure 5, where the course of CO₂ desorption was recorded on a mass spectrometer (mass contributions *m/z* = 16 were collected). To avoid damaging the mass spectrometer detector, the temperature rise was finished at about 650 °C. The CO₂-TPD profiles of the examined samples represent all types of basic sites—weak, medium, and strong—but a strict separation was not possible—even more than three types of sites can be noticeable in some cases. The catalyst with the lowest concentration of K (sample "5") contained weak and medium basic sites with some amount of very strong basic sites with a temperature maximum at 600 °C. The "4" catalyst, having a slightly higher concentration of K (0.9 wt.%) than sample "5", exhibited very similar profiles of CO₂ desorption. A further increase in K concentration (2.4 wt.%) led to a higher amount of medium basic sites with a maximum desorption at 220 °C (Table 5), but stronger basic sites corresponding to CO₂ desorption at about 350 °C also appeared in the catalyst. An even higher concentration of potassium in the catalyst (8.2 wt.%) resulted

in a substantial increase of the amount of medium and stronger basic sites desorbing at 275 and 444 °C, respectively. The catalyst with very a high concentration of potassium (18.9 wt.%) exhibited quite different CO₂ desorption profiles: Weak and medium basic sites completely disappeared, and only very strong basic sites remained. The BP catalyst prepared by the K-impregnation of wet cake method (2.1 wt.% K) exhibited a similar amount of basic sites in the range of 25–650 °C as sample “3”, having 2.4 wt.% K (Table 5). However, the CO₂ desorption course of the BP catalyst differed slightly from those of the other catalysts (Figure 5), as it showed a higher amount of stronger and very strong basic sites characterized by CO₂ desorption at T_{max} of about 277 and 630 °C, respectively.

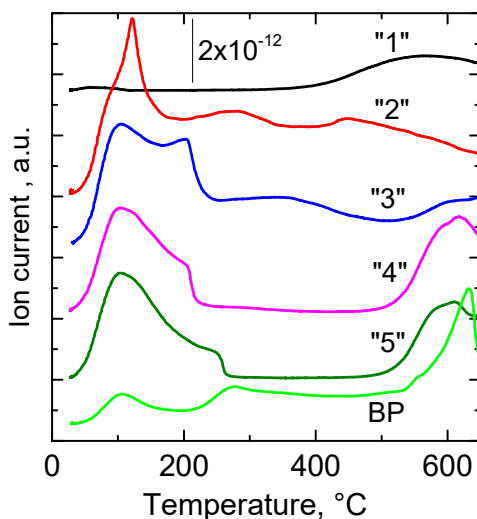


Figure 5. CO₂-TPD desorption profiles (in A) of the catalysts (calcined for 4 h at 500 °C) containing various amounts of K.

2.2.6. FTIR

Fourier transform infrared spectroscopy (FTIR) can identify various kinds of molecular bonds present in solid samples. The FTIR data of both the examined dried Co–Mn–Al–K hydrotalcite-like precursors and their calcined analogs are shown in Figure 6. In the FTIR spectra of the dried samples, a band at 1355 cm^{−1} dominated, which is ascribed, according to literature [27], to characteristic CO₃ antisymmetric stretching mode vibration. Its presence in the spectra, together with the presence of the OH stretching mode band at 3435 cm^{−1} (not shown) confirms the formation of hydrotalcite-like compounds during precipitation. In all dried samples, there was also the vibration at 860 cm^{−1}, which corresponds, according to literature, also to the K₂CO₃ out-of-plane bending mode [27]. In the case of sample “1”, a band at 822 cm^{−1} corresponded to KNO₃ and/or Al(NO₃)₃ out-of-plane bending mode. A very wide band appeared at 738 cm^{−1}, which can indicate a metal-to-oxygen bond of very small particles. The band can be ascribed to Al–O vibrations in AlOOH, which could be also formed during metal nitrates precipitation. In the region below 600 cm^{−1}, other metal–oxygen bonds also occurred that cannot be ascribed with certainty.

The FTIR spectra of the calcined samples show unique bands at 657 cm^{−1} and approximately 552 cm^{−1}. Both bands can indicate the presence of Co₃O₄, MnO₂, Mn₃O₄ [28], or cryptomelane [29]. Potter et al. [29] attributed a band at 550 cm^{−1} unambiguously to cryptomelane. Though Co₃O₄ shows the closest IR spectrum to those of analyzed samples, the presence of cryptomelane cannot be excluded. Samples “1” and “2”, with the highest concentration of K, also exhibited KNO₃ vibrations. By comparing the spectra with references, the presence of other substances in the catalysts was excluded. KNO₃ bands split into pairs 824 and 1372 cm^{−1} and pairs 833 and 1347 cm^{−1}, respectively, the first pair being more tightly bound, i.e., worse washed out. This splitting of the bands could be explained by the different structure of KNO₃ (calcite—trigonal and aragonite—orthorhombic). The aragonite structure arises from the violation of symmetry (for example by adsorption, change of environment, or recrystallization),

thereby increasing the intensity of the originally inactive vibrations [30]. The calcined BP catalyst prepared by bulk promotion exhibits, in principle, the same IR spectrum as the K-precipitated catalyst having nearly the same K concentration (sample “3”). However, it showed slightly higher amount of nitrates (bands at about 1350 and 830 cm^{-1}).

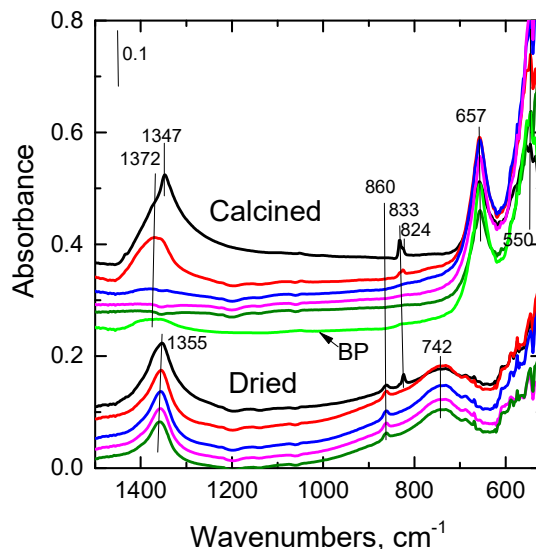


Figure 6. FTIR data of the dried and calcined K-precipitated Co–Mn–Al–K mixed oxides and K-impregnated wet cake catalyst (BP) catalyst. Curves from top to bottom: Samples “1”, “2”, ..., “5”.

2.2.7. Surface Composition

The surface compositions in the near-surface region and chemical state of the elements of the fresh K-precipitated catalysts were determined by XPS. As the catalytic measurements proceeded at reaction temperatures 650–700 °C, the catalysts were calcined at 700 °C, and, therefore, the properties of the catalysts’ surfaces calcined at 700 °C were examined. The surface concentrations of the elements were determined from the intensities (peak areas) divided by the corresponding response factor [31]. Carbon tape used for fixing of the samples to the holder manifested itself in a relatively high concentration of C (28–35 at. %) (Table 6). Nevertheless, the calibration of the spectra was carried out according to carbon (284.8 eV). In the fresh K-precipitated samples calcined at 700 °C, 44 at. % of O, 8.7 at. % of Co, 3.3 at. % of Mn, 7.2 at. % of Al, and 3.3 at. % of K—in average—were determined (Table 7). The gradual washing of the precursor with distilled water resulted in a progressive decrease of K concentration and, at the same time, in the enhancement of other metal elements in the catalysts. In all catalysts, manganese occurred in a higher oxidation state, very likely as Mn^{+4} , most likely MnO_2 . Aluminum looked very similar in all samples and was probably Al_2O_3 , though the position of the peak is shifted slightly in comparison with published data. In all samples, potassium occurred in an identical form, very likely bounded to metal oxide (KMnO_4 , $\text{KMn}_8\text{O}_{16}$, KCoO_2 , or a similar compound).

The deconvolution of oxygen spectra revealed two peaks (Table 6) with binding energies of about 529.8 and 531.5 eV. The first one at 529.8 eV can be ascribed to metal oxide (lattice oxygen O^{2-}), and the second at 531.5 eV can be ascribed to the adsorbed surface oxygen bound to metal oxides as O_2^- , O^- , or OH^- species.

In contrast to the K-precipitated catalysts, the K-impregnated wet cake (BP) catalyst calcined at 700 °C exhibited 54 at. % of O, 13.7 at. % of Co, 6.1 at. % of Mn, 8.1 at. % of Al, 5.2 at. % of K, and 12.5 at. % of C (Table 6). It is obvious that the surface Co concentration of the BP catalyst was the highest of all examined catalysts, and the K concentration was the second highest. The distinctions are certainly a result of different preparation procedures of the examined catalysts.

Table 6. Concentration of elements [at. %] in both the BP catalyst and the K-precipitated catalysts calcined at 700 °C and the relative quantum of two forms of oxygen in the decomposed of O 1s peak.

Sample	Co 2p At. %	Mn 2p At. %	Al 2p At. %	C 1s At. %	K 2p At. %	O 1s At. %	O 1s eV (rel. %)	O 1s eV (rel. %)
"1"	6.8	2.4	5.1	28.7	10.1	46.9	529.7 (45.8)	531.5 (54.2)
"2"	9.5	2.9	6.2	34.8	3.6	43.1	529.7 (63.5)	531.5 (36.5)
"3"	9.1	4.0	7.0	34.1	2.4	43.5	529.7 (67.8)	531.5 (32.2)
"4"	9.0	3.5	8.6	35.9	0.5	42.7	529.8 (56.7)	531.4 (43.3)
"5"	9.1	3.7	9.2	32.5	0.1	45.3	529.9 (59.1)	531.5 (40.8)
BP	13.7	6.1	8.1	12.5	5.2	54.4	530.0 (84.5)	531.7 (15.5)

The surface and bulk concentrations of the main catalyst components (in wt.%) are summarized in Table 7. A comparison of both groups of values indicates that the surface of the catalyst prepared by calcination of the non-washed K-precipitated catalyst precursor was substantially enriched by aluminum (2.5 times) and only slightly enriched by manganese and potassium (in both cases 1.2 times) at the expense of cobalt, which was reduced 0.8 times. The gradual washing of the precipitates by water led to the further enrichment of the catalyst surface by aluminum (3.3 times) at the expense of potassium. Manganese and cobalt surface concentrations practically did not change with the washing of the precipitates. Potassium concentration on the surface and in the bulk also practically did not differ with washing, which indicates the relatively high stability of potassium in the K-precipitated catalyst at calcination temperatures around 700 °C.

Somewhat different relation of surface and bulk composition can be observed for the BP catalyst. The surface concentration of K was more than four times higher than the bulk, while the surface concentration of cobalt was about two thirds of the bulk. Additionally in this sample, surface is enriched by aluminum. The data indicates that the addition of KNO₃ to the wet cake of Co–Mn–Al hydrotalcite-like led to the preferential adsorption of K to Co.

Table 7. Surface concentrations of active components in the calcined catalysts obtained by X-ray photoelectron spectrometry (XPS) in wt.% (in parenthesis there are concentrations of metals in wt.% determined by chemical analysis).

Sample	K	Co	Mn	Al	O
"1"	22.1 (18.9)	21.8 (28.2)	7.2 (6.0)	7.6 (3.0)	41.3 (43.9)
"2"	8.2 (8.2)	32.6 (40.0)	9.2 (8.8)	9.7 (4.0)	40.2 (39.0)
"3"	5.5 (2.4)	30.8 (45.4)	12.8 (10.2)	10.9 (4.7)	40.1 (37.3)
"4"	1.1 (0.9)	32.1 (46.8)	11.6 (10.2)	14.0 (4.7)	41.3 (37.4)
"5"	0.3 (0.6)	31.2 (45.6)	11.9 (9.9)	14.4 (4.4)	42.1 (39.5)
BP	8.3 (2.1)	33.1 (48.9)	13.9 (11.2)	9.0 (5.1)	35.7 (32.7)

2.2.8. Species-Resolved Thermal Alkali Desorption (SR-TAD)

The stability of alkali metals on the catalyst surface was studied by species resolved thermal alkali desorption (SR-TAD). The results of two selected samples prepared by two different methods of K promotion and calcined at 700 °C were compared (Figure 7). Since desorption of K atoms was more significant than the potassium desorption in the form of ions, only desorption of alkali metal atoms (atom fluxes) during heating was observed.

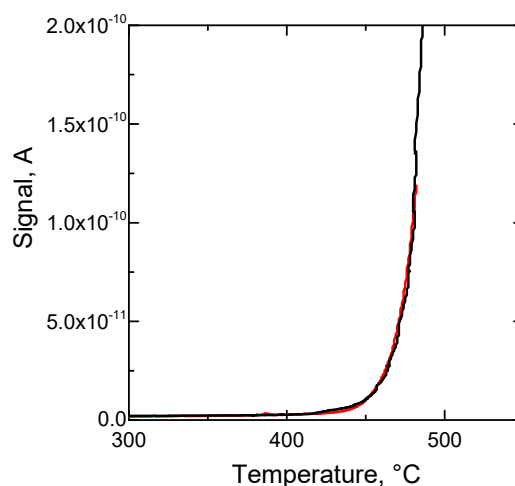


Figure 7. Atomic K desorption flux as a function of temperature during heating. Black line: K-precipitated sample “2”, red line: BP catalyst, both calcined prior to measurements at 700 °C/4 h.

It is obvious from the temperature-dependent changes of atomic fluxes (Figure 9) that potassium desorption already occurs at temperatures higher than 450 °C, what means that the desorption of alkali metals is possible at the temperatures used for calcinations and during NO direct decomposition testing. The same non-monotonic curves in the desorption signal with rising temperature were observed for both samples, which indicates that the potassium promoter leaves the surface through a single energy barrier, and the distribution of the promoter on the catalysts surface here was homogenous [32]. Since the dependence was the same for both differently prepared samples, the resulting potassium surface state should be the same in both samples.

Interestingly, the K atomic desorption flux profiles were different for heating and cooling periods (not shown) for both samples. A slightly higher desorption flux during cooling was observed. A higher signal during cooling than during heating means that some potassium was segregated on the catalyst surface during heating. Different flux profiles obtained during heating and cooling point to potassium migration processes which took place during the measurement—diffusion inside the bulk, agglomeration on the surface, and thermal desorption [33]. These processes probably also take place during the catalytic reaction.

2.2.9. Activity of the Catalysts in Decomposition of NO

The effect of potassium amount on the catalytic activity of K promoted Co–Mn–Al mixed oxides in direct NO decomposition was studied over the catalysts prepared by coprecipitation of metal nitrates with a K_2CO_3/KOH solution and compared with the activity of the catalyst prepared by the K-impregnation of wet cake. Catalytic activity was determined over the catalysts calcined for 4 h at 700 °C. We found that activity of all samples slightly increased with the increasing time-on-stream. After 13 h, the activity reached stable values. In this initial period of catalyst testing, potassium was likely migrating from the interior of the catalyst grains to their surface. The steady state NO conversions obtained over the catalysts with various K concentrations at 650 and 700 °C are depicted in Figure 8 in comparison with that of the catalyst BP prepared by the K-impregnation of wet cake [19]. The highest conversion of NO (ca 61%) was observed at 700 °C in the presence of the catalyst containing about 8 wt.% K prepared by the coprecipitation of metal nitrates with a K_2CO_3/KOH solution. Lower and higher K content led to the decrease of NO conversion, and, for K content lower than 0.6 wt.%, NO catalytic decomposition was not observed at all. The promotional effect of K has already been well described in the case of N_2O catalytic decomposition over K-promoted Co–Mn–Al mixed oxides [34]. Potassium, due to its low ionization potential, enables the charge transfer to the transition metal cations, inducing an electric field gradient at the surface generated by the resulting dipole and the

modification of the density of states characteristics. When K content was higher than the optimal amount, depolarization occurred, leading to the decrease of NO conversion.

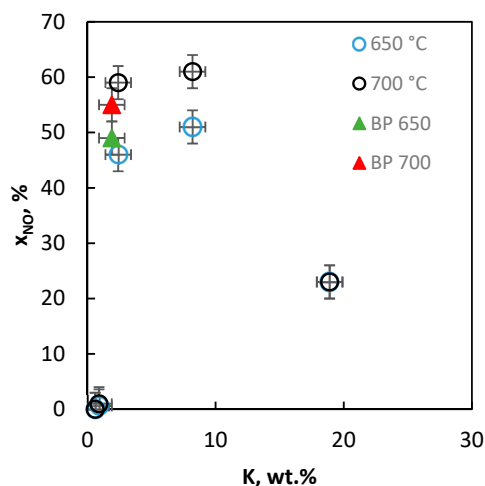


Figure 8. Dependence of nitric oxide (NO) conversion in direct NO decomposition over K-precipitated Co-Mn-Al oxide (circles) and K-impregnated wet cake (BP—triangles) Co-Mn-Al oxide catalysts on the concentration of potassium for two reaction temperatures. Reaction conditions: 1000 ppm NO balanced by N_2 , $T = 650$ or 700 °C, $\text{WHSV} = 6000 \text{ mL g}^{-1} \text{ h}^{-1}$.

2.2.10. Effect of O_2 and CO_2 in the Reactant on Catalytic Activity

As flue gases from power plants contain some amount of other constituents, not only NO, the effect of oxygen or CO_2 in the reactant on catalytic activity was studied with the most active sample “2” at reaction temperature 700 °C. The concentration of both components varied gradually from 1 to 10 molar %. The obtained results are depicted in Figure 9. The effect of both added reaction components was similar: The highest decrease in activity was observed after the addition of their lowest concentration (1 mol %)—however, the effect on initial catalytic activity decrease differed: The presence of O_2 caused a slower decrease in activity than CO_2 . However, higher concentrations of O_2 or CO_2 (about 4 mol %) showed a nearly identical decrease in catalytic activity. Very likely, the adsorption of both components either blocked adsorption of NO or slowed down desorption of N_2 and O_2 .

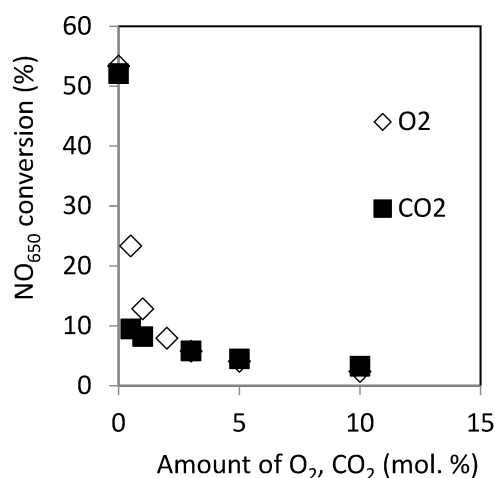


Figure 9. Dependence of NO conversion in direct decomposition at 650 °C on the amount of O_2 or CO_2 in the reaction mixture for sample “2” having 8.2 wt.% of K. Reaction conditions: 1000 ppm NO balanced by N_2 , $T = 700$ °C, $\text{WHSV} = 6000 \text{ mL g}^{-1} \text{ h}^{-1}$.

3. Discussion

In this paper, a method of the preparation of the potassium promoted Co–Mn–Al mixed oxide catalyst (K-precipitated) was examined. An alternative method of the preparation of potassium promoted Co–Mn–Al mixed oxide consists of the precipitation of metal nitrates with potassium salts (K_2CO_3/KOH) and of the consecutive gradual washing of the precipitate to obtain a specific concentration of K in the calcined catalyst. The application of the preparation procedure led to the catalysts with various concentration of potassium whose physical–chemical properties were studied. Their properties were compared with those of the catalyst prepared by the K-impregnation wet cake method.

As shown in the XRD profiles of the calcined catalysts, both kinds of catalysts with similar K content, the K-precipitated sample “3” and BP, contained identical crystallographic phases of the compounds (Figure 2). However, the dimension of coherent domain of spinel (L_d) was somewhat higher for the BP catalyst (9.3 nm) than for the K-precipitated catalyst with a corresponding K amount (6.6 nm)—see Table 4. This finding reflects a slightly lower surface area and a higher total volume of pores and of micropores of the BP catalyst.

FTIR measurements proved that the BP catalyst comprises more nitrates than the K-precipitated catalyst of corresponding composition (Figure 6). It could not cohere with a slightly lower concentration of potassium in the BP catalyst (2.1 wt.%) than the compared catalyst (2.4 wt.%). The phenomenon had to correspond with the way of KNO_3 addition: In the case of the BP catalyst, KNO_3 was likely deposited on the surface of the primary precipitated particles, while, in the case of the washed K-precipitated catalysts, KNO_3 was included in the structure of the hydroxalcalite-like compound formed during the precipitation of metal nitrates with a solution of K_2CO_3/KOH .

The presence of nitrates was reflected in the basicity of the BP catalyst (Figure 5, Table 5), which exhibited a lower amount of stronger basic sites (T_{max} of CO_2 desorption > 220 °C) than the K-precipitated Co–Mn–Al oxide catalyst, with 2.4 wt.% K. Nitrates in the BP catalyst contributed to a higher degree of acidity of the catalyst surface and, thus, to lower basicity.

H_2 -TPR did not show any significant difference in the reducibility of both kinds of the compared catalysts. The catalyst with ca 8 wt.% of K exhibited the lowest T_{max} temperatures in the TPR curves of all samples, thus indicating the easiest reducibility of the transition metals mixed oxides. The reduction profile of the catalyst prepared by K-impregnation of wet cake (BP) was similar to that of sample “5”, which had a three times lower concentration of potassium and therefore documented the lower redox properties of the BP catalyst.

A comparison of the XPS and chemical analysis data for the K-precipitated and BP catalysts led to the following statement: The K-precipitation method of Co–Mn–Al catalysts made uniform distribution of potassium in the catalyst particles possible, while the K-impregnated wet cake method caused the significant enrichment of the catalyst surface by potassium at the expense of cobalt. That is why the optimum concentration of potassium (determined by chemical analysis), which was necessary to obtain the highest NO conversion, was lower [19] in the case of BP preparation method (about 2 wt.%) than in the case of the K-precipitation method (about 8 wt.%).

The catalytic activity of the K-precipitated Co–Mn–Al oxide catalysts in direct decomposition of NO varied with the concentration of K in the solids. It went through maximum at about 8 wt.% K in the solid and decreased when lower and higher K concentrations were present in the catalysts than this optimum value (Figure 8). The BP catalyst exhibited a slightly lower catalytic activity, caused, very likely, by a slightly lower surface area of the catalyst or lower amount of basic sites on the catalyst surface, which substantially affected the sorption of NO on the catalyst surface and/or a slightly lower reducibility of the catalyst.

In Figure 10, the dependence of NO conversions on number of K atoms per nm^2 of the catalyst is depicted. The optimum number of K atoms on the surface is around 10 atoms per nm^2 . With a decrease of this number, the conversion of NO sharply decreased, and, at the value of 1 atom per nm^2 conversion of NO approached zero. On the other hand, the decrease in NO conversion with an

increasing number of atoms per nm^2 was not so sharp, and, for that reason, a slightly higher number of K atoms per nm^2 in the case of K concentration fluctuation is better than vice versa.

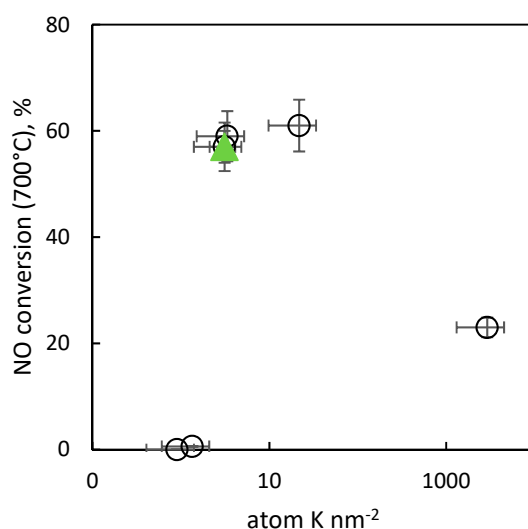


Figure 10. Dependence of NO conversion at 700 °C on the number of K atoms per nm^2 in Co–Mn–Al oxide catalysts. Circles—K-precipitated Co–Mn–Al oxide catalysts, triangles—K-impregnated wet cake Co–Mn–Al oxide (BP) catalyst.

4. Materials and Methods

4.1. Preparation of Catalysts

Co–Mn–Al mixed oxides modified by K were prepared by the co-precipitation of the 210 mL solution of 40 g $\text{Co}(\text{NO}_3)_2 \cdot 6\text{H}_2\text{O}$, 8.7 g $\text{Mn}(\text{NO}_3)_2 \cdot \text{H}_2\text{O}$, and 12.9 g $\text{Al}(\text{NO}_3)_3 \cdot 9\text{H}_2\text{O}$ with the 225 mL aqueous solution of 14.5 g K_2CO_3 and 29.7 g KOH. The solutions were dosed to a vessel equipped with a magnetic Triga stirrer (500 revolutions min^{-1}), in which 100 mL of water were mixed with such an amount of KOH that the solution maintained a $\text{pH} = 10$. The rate of dosing of each solution was ca 1.9 mL/min, the pH of precipitation 10 ± 0.1 , and the temperature was 22 °C. The resulting suspension was mixed for 60 min at laboratory temperature.

Then, the suspension was filtered off, and the precipitate was washed with ca 200 mL of water after removing ca one fifth of the precipitate to obtain different levels of K concentration in the samples. The washed samples were dried for 12 h at 60 °C and calcined at 500 °C. Numbers “1” to “5” labeled the prepared catalysts, with sample “1” having the highest concentration of K and sample “5” having the lowest.

For comparison, a catalyst prepared by the co-precipitation of transition metal nitrates by $\text{Na}_2\text{CO}_3/\text{NaOH}$ solution and the subsequent impregnation of the resulting wet cake by a solution of KNO_3 (K-impregnated wet cake method) was labeled, after drying and calcination, as BP.

4.2. Characterization of the Samples

The content of metals in the prepared catalysts was determined by atomic emission spectroscopy with microwave plasma using an Avio 500 MP-AES (Perkin-Elmer, Chichester, UK) after the dissolution of the samples in diluted (2%) hydrochloric acid.

Phase composition and microstructural properties were determined using an X-ray powder diffraction (XRD) technique. XRD patterns were obtained using a Rigaku SmartLab diffractometer (Rigaku, Tokyo, Japan) equipped with a D/teX Ultra 250 detector. The source of X-ray irradiation was a Co tube ($\text{CoK}\alpha$, $\lambda_1 = 0.178892$ nm, $\lambda_2 = 0.179278$ nm) operated at 40 kV and 40 mA. Incident and diffracted beam optics were equipped with 5° Soller slits; incident slits were set up to irradiate a 10×10 mm area of the sample (automatic divergence slits) constantly. The slits on the diffracted beam

were set up to a fixed value of 8 and 14 mm. The powder samples were gently grinded using an agate mortar before analysis, pressed using microscope glass in a rotational sample holder, and measured in reflection mode (Bragg–Brentano geometry). The samples were rotated (30 rpm) during the measurement to eliminate the preferred orientation effect. The XRD patterns were collected in a 2θ range 5° – 90° with a step size of 0.01° and speed of $0.5 \text{ deg}\cdot\text{min}^{-1}$. The measured XRD patterns were evaluated using the PDXL 2 software (version 2.4.2.0) and compared with the PDF-2 database issued by ICDD, released in 2015. Nitrogen physisorption on catalyst powders (grain size 0.16–0.32 mm) was performed using an ASAP 2020 Micromeritics instrument (Norcross, Atlanta, GA, USA) after degassing at 105°C for 24 h at 1 Pa vacuum. The adsorption–desorption isotherms of nitrogen at 77 K were evaluated by the standard Brunauer–Emmett–Teller (BET) procedure [35] for the p/p_0 range = 0.05–0.25 to calculate the specific surface area S_{BET} . Mesopore surface areas, S_{meso} , and micropore volume, V_{micro} , were determined by the t -plot method [36]. The total pore volume, V_{total} , was determined from the nitrogen adsorption isotherm at maximum p/p_0 (~ 0.995). The pore-size distribution (pore radius 10^0 – 10^2 nm) was evaluated from the adsorption branch of the nitrogen adsorption–desorption isotherm by the Barrett–Joyner–Halenda (BJH) method [37], assuming a cylindrical pore geometry. The Lecloux–Pirard standard isotherm [38] was used for the t -plot and for the pore-size distribution evaluation.

Temperature programmed reduction (H_2 -TPR) measurements were performed with a H_2/N_2 mixture (10 mol % H_2), flow rate $50 \text{ mL}\cdot\text{min}^{-1}$ and a linear temperature increase of $20^\circ\text{C}\cdot\text{min}^{-1}$ up to 900°C . Changes in H_2 concentration were detected with a catharometer. A reduction of grained CuO (0.160–0.315 mm) was performed to calculate the absolute values of the hydrogen consumed during reduction of the samples.

The temperature-programmed desorption of CO_2 (CO_2 -TPD) was carried out to examine basic properties of the catalysts surface. The measurements were accomplished with a 0.050 g sample in the temperature range of 20 – 900°C , with helium as a carrier gas and CO_2 as the adsorbing gas. Prior to the CO_2 -TPD measurement, the sample was heated in helium from 25 to 500°C with a temperature ramp of $20^\circ\text{C}\cdot\text{min}^{-1}$; then, the sample was cooled in helium to 25°C . Ten doses of CO_2 , $840 \mu\text{L}$ each, were applied to the catalyst sample at 30°C before flushing with He for 1 h and heating at a rate of $20^\circ\text{C}\cdot\text{min}^{-1}$. The composition of the gases evolved during the experiments was determined by a mass spectrometer (Balzers, Pfeiffer Vacuum, Asslar, Germany). The following mass contributions m/z were collected: 2 - H_2 and 44 - CO_2 . The spectrometer was calibrated by dosing the known amount of CO_2 into the carrier gas (He) in every experiment. The H_2 -TPR and CO_2 -TPD experiments were evaluated using OriginPro 8.0 software with an accuracy of $\pm 5\%$.

The thermal decomposition of dried materials was conducted by heating the 10 mg of samples to 700°C at a rate of $2^\circ\text{C}/\text{min}$, using a NETZSCH TG 209 F1 Libra (Selb, Germany) recording microbalances in a stream of inert gas (Ar) at a flow rate $50 \text{ mL}/\text{min}$. The sample was heated in the oven, the output of which was regulated by a programmable digital temperature controller. The flow of carrier gas was controlled by electronic mass flowmeters.

A Nicolet Model 360 Avatar FT-IR spectrometer (Analytical Instruments Brokers LLC, Golden Valley, MN, U.S.A.) was used in an attenuated total reflection (ATR) mode to obtain the spectra from catalysts between 360 and 4000 cm^{-1} (resolution 1.93 cm^{-1} , 300 scans, 1 s per scan) when the powder was pressed against ZnSe crystal (working range between 508 and 4000 cm^{-1}). All spectra were obtained at laboratory temperature ($\sim 22^\circ\text{C}$) and atmospheric pressure.

The thermal stability of the alkali metal promoters was investigated by the species resolved thermal alkali desorption (SR-TAD) method. The experiments were carried out in a vacuum apparatus with a background pressure of 10^{-7} kPa. The samples in the form of wafers (13 mm diameter, 200 mg weight) were heated at the rate of $5^\circ\text{C}\cdot\text{min}^{-1}$ from room temperature up to 650°C in a stepwise voltage-controlled mode. Then, they were cooled down at the same rate. The desorption flux of potassium atoms was determined by means of a surface ionization detector, consisting of a platinum wire heated by a current of 2.2 A, to approximately 1000°C , with a positive potential of $+120 \text{ V}$ causing the ionization of the desorbed atoms and their acceleration towards the collector. During the

measurements, the samples were biased with a positive potential +5 V to quench the thermal emission of electrons. In this way, the possibility of the reneutralization of ions by thermal electrons outside the surface was effectively eliminated. The resulting positive current was directly measured with a Keithley 6512 digital electrometer.

Superficial elemental analyses were performed by XPS (X-ray photoelectron spectrometry ESCA 3400, Kratos, Manchester, UK) at a base pressure better than 5×10^{-7} Pa, using the polychromatic Mg X-ray source (Mg K α , 1253.4 eV). The composition of the elements was determined without any annealing. For the spectra, the Shirley background was subtracted, and the elemental compositions of layers were calculated from the corresponding areas.

The catalytic decomposition of NO to N₂ and O₂ was performed in an integral fixed bed stainless steel reactor of 5 mm internal diameter (650 °C or 700 °C, 0.5 g, 49 mL min⁻¹). To some catalytic runs, oxygen (0–10 mol%) was added to an inlet gas composed of 1000 ppm NO in N₂. The catalysts (fraction 0.16–0.316 mm) pre-calcined at 700 °C were activated in 50 mL of N₂ + O₂ min⁻¹ (101325 Pa, 20 °C) for 1 h at 650 °C. Then, the NO catalytic decomposition at 650 °C was measured at least for 15 h. After this period, when a stable performance was observed, the temperature dependence of conversion was launched with cooling rate of 5 °C min⁻¹, and the catalysts activity was measured for 3 h at each temperature (640 °C, 620 °C, 600 °C, 580 °C, and 560 °C). After the conversion curve measurement, the reactor was heated back to 650 °C in order to check the stability of the catalyst. In case the performance was stable, the catalyst was heated to 700 °C, and the steady state conversion at 700 °C was measured. When the oxygen was added to the inlet mixture, it took 1 h at minimum to achieve steady state performance. Infrared analyzers for the online analysis of NO (Ultramat 6, Siemens, Karlsruhe, Germany) and N₂O (Sick) were used. During all measurements, no N₂O and no NO₂ were detected, as proven by the low-temperature NO₂/NO catalytic convertor (TESO Ltd.). The activity of the catalysts was determined as conversions of NO from the relation $X_{\text{NO}} = (c_{\text{NO}}^0 - c_{\text{NO}}) / c_{\text{NO}}^0$, where X_{NO} is NO conversions, c_{NO}^0 is the initial NO concentration, and c_{NO} is the NO concentration at reactor outlet.

5. Conclusions

The investigated process of the K promoted Co–Mn–Al catalyst preparation consisting of the precipitation of transition metal nitrates with a solution of K₂CO₃/KOH is simpler than the other possible ways of preparation, e.g., the K-impregnation of wet cake method. When using the examined process of preparation, it is possible to obtain a catalyst with a desired K concentration in the solids without any additional preparation steps. The concentration of potassium affected catalytic activity of the K-precipitated catalysts in direct NO decomposition, the highest being at ca 8 wt.% of K, while that of the K-impregnated wet cake samples was about 2 wt.%. We believe that the incorporation of potassium into the catalyst particle structure positively influences catalyst stability, as the potassium inside the catalyst particles serves as its reservoir when it desorbs from the surface during catalytic reaction.

Supplementary Materials: The following are available online at <http://www.mdpi.com/2073-4344/9/7/592/s1>, Figure S1: Diffraction patterns of the dried K-precipitated Co–Mn–Al compounds containing various amounts of potassium. H – hydrotalcite-like compounds, R – rhodochrosite, K – KNO₃, Figure S2: Adsorption-desorption isotherms of nitrogen for K-precipitated Co–Mn–Al mixed oxides containing various amounts of potassium in wt. %: curve 2 – 8.20, curve 3 – 2.39, curve 4 – 0.92, curve 5 – 0.60, Table S1: Details of the preparation method and concentration of K and Na (mg/L) in filtrate and washing waters.

Author Contributions: Conceptualization, K.J.; methodology, K.J. and K.P.; validation, T.B., L.O., A.M., A.K. (Andrzej Kotarba), and K.J.; investigation, J.B., T.B., K.P., K.K., A.K. (Anna Klegová), A.M., V.J., and M.K.; data curation, T.B., K.P., K.K., J.B., A.K. (Anna Klegová), and M.K.; writing—original draft preparation, K.J.; writing—review and editing, K.J. and K.P.; supervision, L.O.; project administration, K.P., L.O., and K.J.

Funding: The authors thank Czech Science Foundation (project No. 18-19519S) for financial support. The work was also supported from ERDF “Institute of Environmental Technology – Excellent Research” (No. CZ.02.1.01/0.0/0.0/16_019/0000853). Experimental results were accomplished by using Large Research Infrastructures ENREGAT and CATPRO supported by the Ministry of Education, Youth and Sports of the Czech Republic under projects No. LM2018098 and No. LM2015039.

Acknowledgments: The authors thank L. Soukupová for the chemical analysis of the samples and H. Šnajdaufová for the measurement of porous structure of the catalysts.

Conflicts of Interest: The authors declare no conflict of interest.

References

1. Bu, Y.F.; Ding, D.; Gan, L.; Xiong, X.H.; Cai, W.; Tan, W.T.; Zhong, Q. New insights into intermediate-temperature solid oxide fuel cells with oxygen-ion conducting electrolyte act as a catalyst for NO decomposition. *Appl. Catal. B* **2014**, *418*, 158–159. [[CrossRef](#)]
2. Janssen, J. *Environmental Catalysis—Stationary Sources, Environmental Catalysis*; Wiley-VCH Verlag GmbH: Weinheim, Germany, 2008; pp. 119–179.
3. Li, J.; Chang, H.; Ma, L.; Hao, J.; Yang, R.T. Low-temperature selective catalytic reduction of NO_x with NH₃ over metal oxide and zeolite catalysts—A review. *Catal. Today* **2011**, *175*, 147–156. [[CrossRef](#)]
4. Javed, M.T.; Irfan, N.; Gibbs, B.M. Control of combustion-generated nitrogen oxides by selective non-catalytic reduction. *J. Environ. Manage.* **2007**, *83*, 251–289.
5. Wu, Y.; Dujardin, C.; Lancelot, C.; Dacquain, J.P.; Parvulescu, C.M.; Henry, C.R.; Neisius, T. Catalytic abatement of NO and N₂O from nitric acid plants: A novel approach using noble metal-modified perovskites. *J. Catal.* **2015**, *328*, 236–247. [[CrossRef](#)]
6. Haneda, M.; Hamada, H. Recent progress in catalytic NO decomposition. *C. R. Chim.* **2016**, *19*, 1254–1265. [[CrossRef](#)]
7. Falsig, H.; Bligaard, T. Trends in catalytic NO decomposition over transition metal surfaces. *Top. Catal.* **2007**, *45*, 117–120. [[CrossRef](#)]
8. Brown, W.A.; King, D.A. NO Chemisorption and Reactions on Metal Surfaces: A New Perspective. *J. Phys. Chem. B* **2000**, *104*, 2578–2595. [[CrossRef](#)]
9. Falsig, H.; Bligaard, T.; Christensen, C.H.; Nørskov, J.K. Direct NO decomposition over stepped transition-metal surfaces. *Pure Appl. Chem.* **2007**, *79*, 1895–1903. [[CrossRef](#)]
10. Wu, Z.; Xu, L.; Zhang, W.; Ma, Y.; Yuan, Q.; Jin, Y.; Yang, J.; Huang, W. Structure sensitivity of low-temperature NO decomposition on Au surfaces. *J. Catal.* **2013**, *304*, 112–122. [[CrossRef](#)]
11. Haneda, M.; Kintaichi, Y.; Hamada, H. Catalytic active site for NO decomposition elucidated by surface science and real catalyst. *Appl. Catal. B* **2005**, *55*, 169–175. [[CrossRef](#)]
12. Bonzel, H.P.; Bradshaw, A.M.; Ertl, G. *Physics and Chemistry of Alkali Metal Adsorption*; Elsevier: Amsterdam, The Netherlands, 1989.
13. Mross, W.D. Alkali doping in heterogeneous catalysis. *Catal. Rev.* **1983**, *25*, 591–637.
14. Niemantsverdriet, J.W. *Spectroscopy in Catalysis*; Wiley-VCH Verlag GmbH & Co.: Weinheim, Germany, 2007; p. 271.
15. Pacultová, K.; Draščíková, V.; Chromčáková, Ž.; Bílková, T.; Mamulová-Kutláková, K.; Kotarba, A.; Obalová, L. On the stability of alkali metal promoters in Co mixed oxides during direct NO catalytic decomposition. *Mol. Catal.* **2017**, *428*, 33–40. [[CrossRef](#)]
16. Wang, Y.; Hu, X.; Zheng, K.; Zhang, H. Effect of precipitants on the catalytic activity of Co–Ce composite oxide for N₂O catalytic decomposition. *Reac. Kinet. Mech. Cat.* **2018**, *123*, 707–721. [[CrossRef](#)]
17. Zhang, Q.; Luo, J.; Vilenko, E.; Steven, L.; Suib, S.L. Synthesis of cryptomelane-type manganese oxides by microwave heating. *Chem. Mater.* **1997**, *9*, 2090–2095. [[CrossRef](#)]
18. Kovanda, K.; Rojka, T.; Dobešová, J.; Machovič, V.; Bezdička, P.; Obalová, L.; Jiráťová, K.; Grygar, T. Mixed oxides obtained from Co and Mn containing layered double hydroxides: Preparation, characterization, and catalytic properties. *J. Solid State Chem.* **2006**, *179*, 812–823. [[CrossRef](#)]
19. Pacultová, K.; Bílková, T.; Klegová, A.; Karásková, K.; Fridrichová, D.; Martaus, A.; Jiráťová, K.; Kiška, T.; Balabánová, J.; Koštejn, M.; et al. Direct NO decomposition over K-promoted Co-Mn-Al mixed oxides. *Catalysts* **2019**, *9*. (submitted).
20. Klyushina, A.; Pacultová, K.; Karásková, K.; Jiráťová, K.; Ritz, M.; Fridrichová, D.; Volodarskaja, A.; Obalová, L. Effect of preparation method on catalytic properties of Co-Mn-Al mixed oxides for N₂O decomposition. *J. Mol. Catal. A Chemical.* **2016**, *425*, 237–247. [[CrossRef](#)]

21. Santos, V.P.; Soares, O.S.G.P.; Bakker, J.J.W.; Pereira, M.F.R.; Órfão, J.J.M.; Gascon, J.; Kapteijn, F.; Figueiredo, J.L. Structural and chemical disorder of cryptomelane promoted by alkali doping: Influence on catalytic properties. *J. Catal.* **2012**, *293*, 165–174. [CrossRef]
22. Becerra, M.E.; Arias, N.P.; Giraldo, O.H.; López Suárez, F.E.; Illán Gómez, M.J.; Bueno López, A. Soot combustion manganese catalysts prepared by thermal decomposition of KMnO_4 . *App. Catal. B Environ.* **2011**, *102*, 260–266. [CrossRef]
23. Da Costa-Serra, J.F.; Chica, A. Catalysts based on Co-Birnessite and Co-Todorokite for the efficient production of hydrogen by ethanol steam reforming. *Intern. J. Hydrog. Energy* **2018**, *43*, 16859–16865. [CrossRef]
24. Obalová, L.; Karásková, K.; Wach, A.; Kustrowski, P.; Mamulová-Kutlákova, K.; Michalik, S.; Jirátoová, K. Alkali metals as promoters in Co–Mn–Al mixed oxide for N_2O decomposition. *Appl. Catal. A Gen.* **2013**, *462–463*, 227–235. [CrossRef]
25. Imanaka, N.; Masui, T. Advances in direct NO_x decomposition catalysts. *Appl. Catal. A Gen.* **2012**, *431–432*, 1–8. [CrossRef]
26. Smoláková, L.; Frolich, K.; Troppová, I.; Kutálek, P.; Kroft, E.; Čapek, L. Determination of basic sites in Mg–Al mixed oxides by combination of TPD- CO_2 and CO_2 adsorption calorimetry. *J. Therm. Anal. Calorim.* **2017**, *127*, 1921–1929. [CrossRef]
27. Nyquist, R.A.; Nagel, R.O. *Infrared Spectra of Inorganic Compounds*; Academic Press: New York, NY, USA, 1971.
28. Bentley, F.F.; Smithson, L.D.; Rozek, A.L. *Infrared Spectra and Characteristic Frequencies 700–300 cm^{-1} : A Collection of Spectra, Interpretation, and Bibliography*; Interscience: New York, NY, USA, 1986.
29. Potter, R.M.; Rossman, G.R. The tetravalent manganese oxides: Identification, hydration, and structural relationships by infrared spectroscopy. *Am. Mineral.* **1979**, *64*, 1199–1218.
30. Horák, M.; Papoušek, D. *Infračervená spektra a struktura molekul: použití vibrační spektroskopie při určování struktury molekul*, 1st ed.; Academia: Praha, Czech Republic, 1976; 836p.
31. Scofield, J.H. Hartree-Slater subshell photoionization cross-sections at 1254 and 1487 eV. *J. Electron Spectrosc. Relat. Phenom.* **1976**, *8*, 129–137. [CrossRef]
32. Borowiecki, T.; Denis, A.; Rawski, M.; Gołębiowski, A.; Stołeczki, K.; Dmytrzyk, J.; Kotarba, A. Studies of potassium-promoted nickel catalysts for methane steam reforming: Effect of surface potassium location. *Appl. Surf. Sci.* **2014**, *300*, 191–200. [CrossRef]
33. Kaspera, W.; Wojas, J.; Molenda, M.; Kotarba, A. Parallel migration of potassium and oxygen ions in hexagonal tungsten bronze—Bulk diffusion, surface segregation and desorption. *Solid State Ionics* **2016**, *297*, 1–6. [CrossRef]
34. Obalová, L.; Maniak, G.; Karásková, K.; Kovanda, F.; Kotarba, A. Electronic nature of potassium promotion effect in Co–Mn–Al layered double hydroxide on the catalytic decomposition of N_2O . *Catal. Commun.* **2011**, *12*, 1055–1058. [CrossRef]
35. Brunauer, S.; Emmett, P.H.; Teller, E. Adsorption of gases in multimolecular layers. *J. Am. Chem. Soc.* **1938**, *60*, 309–319. [CrossRef]
36. Deboer, J.H.; Lippens, B.C.; Linsen, B.G.; Broekhof, J.C.; Vandenhe, A.; Osinga, T.J. The t-curve of multimolecular N_2 -adsorption. *J. Colloid Interface Sci.* **1966**, *21*, 405–414. [CrossRef]
37. Barrett, E.P.; Joyner, L.G.; Halenda, P.P. The Determination of Pore Volume and Area Distributions in Porous Substances. I. Computations from Nitrogen Isotherms. *J. Am. Chem. Soc.* **1951**, *73*, 373–380.
38. Lecloux, A.; Pirard, J.P. The importance of standard isotherms in the analysis of adsorption isotherms for determining the porous texture of solids. *J. Colloid Interface Sci.* **1979**, *70*, 265–281. [CrossRef]

